

In Situ Signatures of Interchange Reconnection between Magnetic Clouds and Open Magnetic Fields: A Mechanism for the Erosion of Polar Coronal Holes?

Benoit Lavraud · Mathew J. Owens · Alexis P. Rouillard

Received: 30 June 2010 / Accepted: 23 January 2011
© Springer Science+Business Media B.V. 2011

Abstract We outline a method to determine the direction of solar open flux transport that results from the opening of magnetic clouds (MCs) by interchange reconnection at the Sun based solely on *in-situ* observations. This method uses established findings about *i*) the locations and magnetic polarities of emerging MC footpoints, *ii*) the hemispheric dependence of the helicity of MCs, and *iii*) the occurrence of interchange reconnection at the Sun being signaled by uni-directional suprathermal electrons inside MCs. Combining those observational facts in a statistical analysis of MCs during solar cycle 23 (period 1995–2007), we show that the time of disappearance of the northern polar coronal hole (1998–1999), permeated by an outward-pointing magnetic field, is associated with a peak in the number of MCs originating from the northern hemisphere and connected to the Sun by outward-pointing magnetic field lines. A similar peak is observed in the number of MCs originating from the southern hemisphere and connected to the Sun by inward-pointing magnetic field lines. This pattern is interpreted as the result of interchange reconnection occurring between MCs and the open field lines of nearby polar coronal holes. This reconnection process closes down polar coronal hole open field lines and transports these open field lines equatorward, thus contributing to the global coronal magnetic field reversal process. These results will be further constrainable with the rising phase of solar cycle 24.

Keywords Coronal mass ejection · Heliospheric topology · Solar cycle · Solar wind suprathermal electrons

A.P. Rouillard now at: Naval Research Laboratory, Maryland, USA.

B. Lavraud (✉) · A.P. Rouillard

Institut de Recherche en Astrophysique et Planetologie, Université de Toulouse (UPS), Toulouse, France
e-mail: lavraud@cesr.fr

B. Lavraud · A.P. Rouillard
UMR 5187, Centre National de la Recherche Scientifique, Toulouse, France

M.J. Owens
The Blackett Laboratory, Imperial College, London, UK

1. Introduction

The Sun's dipolar magnetic field component reverses over a cycle of 11 years. Babcock (1961) provided the first semi-empirical model for the reversal of the polar fields in terms of the evolution of bipolar magnetic regions (BMRs). Since then, many theories of coronal magnetic field evolution have been proposed (Leighton, 1969; Wang, Nash, and Sheeley 1989a, 1989b; Gopalswamy *et al.*, 2003; Schrijver, DeRosa, and Title, 2002; Wang and Sheeley, 2003; Low, 2004; Fisk and Schwadron, 2001; Owens *et al.*, 2007; Dikpati *et al.*, 2010), and no consensus has yet been reached on the exact mechanisms responsible for these cyclical polar field reversals. Nearly all these models have one physical mechanism in common, called interchange reconnection, which occurs when chromospheric magnetic loops (flux ropes, arcades, BMR loops) reconnect with magnetic field lines which stretch out into the interplanetary medium (called ‘open’). Interchange reconnection can lead to the displacement of open magnetic field lines on the Sun because chromospheric loops connect regions of the photosphere that are widely separated (see, *e.g.*, Edmondson *et al.*, 2010; Cohen *et al.*, 2010). The present paper demonstrates in a statistical way that interchange reconnection could play a significant role not only in the evolution of magnetic loops transported by Magnetic Clouds, but also in the evolution of coronal hole open magnetic field lines over the solar cycle through a systematic transport process. Magnetic Clouds (MCs) are magnetic flux rope structures which are expelled from the Sun and expand into the heliosphere. Typical and important properties of MCs are high magnetic field strengths, low ion temperatures (see, *e.g.*, Burlaga *et al.*, 1982; Gosling, 1990), low Mach numbers (see, *e.g.*, Lavraud and Borovsky, 2008), and the frequent presence of bi-directional suprathermal electrons (*e.g.*, Gosling *et al.*, 1987) owing to their closed topology. In Section 2, we review the solar and *in-situ* basic observational facts related to MCs which suggest the occurrence of interchange reconnection. In Section 3 we present the details of our statistical analysis, which is based on *in-situ* measurements of MCs. In the last section, we discuss these results and state the implications for our theoretical understanding of coronal magnetic field evolution.

2. Basic Observational Facts

The solar cycle may be divided into three main phases. A new cycle starts with a “rising phase”; a period during which magnetic flux emerges through the photosphere in the mid-latitude regions ($30\text{--}50^\circ$) in proximity of the polar coronal holes. This phase is associated with an increase in the rate of release of coronal mass ejections (CMEs) and MCs, visible in white-light observations (see, *e.g.*, Webb and Howard, 1994) and measured *in situ* (see, *e.g.*, Cane and Richardson, 2003). This rising phase is marked by the sudden decrease in the surface area occupied by polar coronal holes (*i.e.*, erosion). Figure 1a presents, in a heliocentric latitude versus time format, a synoptic map of the polarity of the photospheric magnetic fields averaged over Carrington longitudes, where black/white areas show latitude bands dominated by inward/outward magnetic fields. The reversal of the polar magnetic fields from one solar minimum to the next is very clear in Figure 1a. Magnetic fields in the northern polar coronal hole were pointing outward in 1996–1997 and then inward in 2005–2006. The sudden disappearance of polar coronal holes can be observed in 1998–1999 during the rising phase of solar activity. The large-scale dipolar magnetic field component changes polarity shortly after the disappearance of the polar coronal holes during the “solar maximum phase”. The “declining phase” is notably longer than the two previous

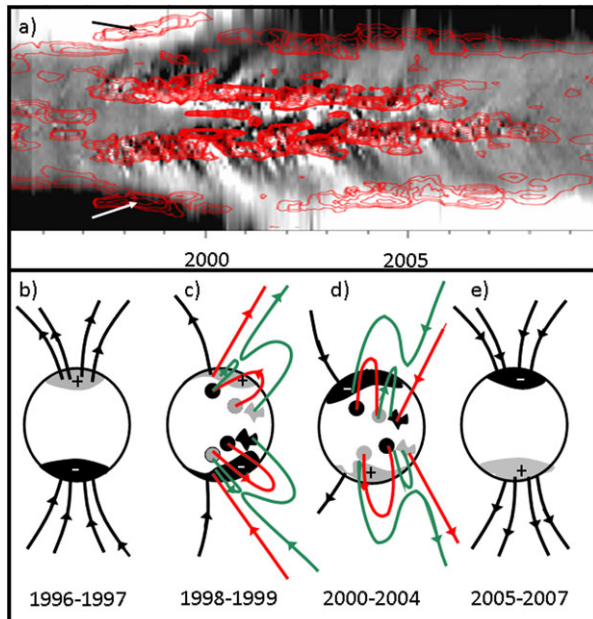


Figure 1 (a) Synoptic map, in a heliocentric latitude versus time format, of the polarity of the photospheric magnetic field averaged over Carrington longitudes (magnetogram from Mount Wilson Observatory measurements), where black/white areas show latitude bands dominated by inward/outward magnetic fields. The gray-scale levels for radial magnetic field are in the range of -4 gauss (black) to 4 gauss (white). Overlaid are contours of coronal green line emissions as estimated using Potential Field Source Surface (PFSS) extrapolations to the observed photospheric magnetic field. Cf. Robbrecht *et al.* (2010) and Wang *et al.* (1997) for details on this method. (b, c, d, e) Schematic of solar magnetic field regions: the northern and southern CHs (signed gray and dark regions at the poles), BMRs with leading pole located equatorward of the trailing pole in each hemisphere (small circles), isolated equatorial coronal holes (irregularly-shaped regions at lower latitudes), and associated MC topologies (colored field-lines). (c) During the solar cycle rising phase, the trailing pole has opposite polarity to the nearby CH. The occurrence of interchange reconnection (assumed here below the Alfvén point) leads to the formation of a small coronal loop that rapidly subsides beneath the photosphere. It also leads to the opening of previously closed MC flux at lower latitude (the positive pole in the northern hemisphere); the process thus has transported open flux from initial CH locations to the lower latitude of the leading BMR/MC pole. (b) A similar process may be envisaged during the declining phase, but the global CH-polarity reversal that occurred at solar maximum changes the scenario so that interchange reconnection may rather lead to poleward open flux transport (after Owens *et al.* (2007) model).

phases; the Sun's magnetic activity (including the CME release rate) gradually decreases. The dipolar magnetic field becomes increasingly well ordered with the Sun's photospheric field characterized by two well-defined and confined polar coronal holes of opposite magnetic polarity in each hemisphere. The new magnetic dipole is by then reversed compared to the previous solar cycle minimum.

The action of Coriolis forces on new magnetic flux emerging through the solar surface gives rise to BMRs with the leading pole located a few degrees equatorward of the trailing pole (Hale and Nicholson, 1925; Wang and Sheeley, 1989; Bothmer and Rust, 1997; Rees and Forsyth, 2003). This is true in both hemispheres. In the case of solar cycle 23 the leading polarity, in the sense of solar rotation, is positive and the trailing one negative in the northern hemisphere. It is opposite in the southern hemisphere. The poleward pole of the BMRs in each hemisphere thus shows a polarity opposite to that of the nearby coro-

nal hole during the rising phase of the cycle. This is sketched in Figure 1c. The emergence of these new-cycle active regions is always associated with changes in polar coronal hole boundaries (moving away from the active regions), as well as sudden chromospheric network enhancements along the edges of the polar coronal holes observed in He I 1083 nm (Sheeley, Wang, and Harvey, 1989). Additionally, strong coronal hole boundary brightening are observed in He II 30.4 nm, Fe XIV 530.3 nm (so-called ‘coronal green line’) and in Fe XII 19.5 nm line (Wang *et al.*, 1997, 2010; Robbrecht *et al.*, 2010). Sheeley, Wang, and Harvey (1989) found, using a potential field source surface model (Wang and Sheeley, 1989), that the enhancements occurred at the footpoints of field lines that were previously open but had now become connected, in the model, to the trailing-polarity sector of the active region. This effect was observed during the rising phase of cycle 22 (Sheeley, Wang, and Harvey, 1989), cycle 23 (Wang *et al.*, 1997; Benevolenskaya, Kosovichev, and Scherrer, 2001; Robbrecht *et al.*, 2010) and during the recent start of cycle 24 (Wang *et al.*, 2010). Sheeley, Wang, and Harvey (1989) suggested that interchange reconnection was the most likely mechanism by which the coronal magnetic field reaches this new configuration. Strong brightness enhancements (situated on the boundary of coronal holes) were observed during a two-year interval centered around 1998. Robbrecht *et al.* (2010) noted that by 11 November 1998 the polar holes had shrunk markedly since the onset of the cycle, and the trailing-polarity flux from the new-cycle active regions had formed connections to the remnant polar-cap fields. The overlaid red color contours in Figure 1a show the estimated (*cf.* Figure 1, caption) coronal green line emissions during solar cycle 23. As mentioned above, this figure shows that the start of the rising phase (1998–1999) corresponds to a clear latitudinal shift in the emission; the peak is inside the polar coronal hole, though at its equatorward edge (*cf.* the arrows in the figure).

During the declining phase the polar coronal holes polarities have changed, but the BMR polarities have not. Thus the BMR pole nearest to the coronal hole has the same polarity as the coronal hole (Figure 1d). Interchange reconnection is thus unlikely to occur there. However, interchange reconnection might occur between remaining isolated coronal holes located more equatorward and nearby the BMRs pole of opposite polarity (*cf.* Figure 1d), thus favoring interchange reconnection and associated poleward transport of open field lines with the appropriate polarity so as to complete the formation of the newly established coronal hole of new polarity. Such a scenario for the declining phase was proposed by Owens *et al.* (2007), and will also be discussed in the present paper.

CME eruptions observed in white-light images are one form of eruptive events which can lift the closed magnetic fields lines of BMRs (rising red loops in Figures 1c and d). MCs measured *in situ* have been directly or indirectly associated with CME eruptions observed in white light. It has been found that the magnetic helicity of BMRs and subsequent MCs are left-handed in the northern hemisphere and right-handed in the southern hemisphere. This rule statistically holds for 75% of MCs (Rust, 1994; Bothmer and Schwenn, 1998; Chandra *et al.*, 2010). Thus the helicity of MCs observed near Earth tells us its hemisphere of origin, independent of the solar cycle. Furthermore, this helicity rule combined with the prevalence of leading positive (negative) poles in the northern (southern) hemisphere during solar cycle 23 preferentially leads to interplanetary MCs with a leading southward magnetic field and a trailing northward magnetic field (SN-polarity), relative to the ecliptic. This rule is also independent of the hemisphere during solar cycle 23. This trend changes with the start of a new cycle; NS-polarity MCs are expected to dominate for cycle 24 (Bothmer and Schwenn, 1998; Mulligan, Russell, and Luhmann, 1998). By analyzing MCs we can therefore analyze the properties of magnetic loops which have emerged near active regions. Owing to their large velocities, suprathermal electrons propagating parallel (or anti-parallel) to the magnetic field

constitute tracers of the heliospheric magnetic topology (see, *e.g.*, Zwickl *et al.*, 1983; Lavraud *et al.*, 2010) and enable us to study the connectivity of MCs at the Sun. Observation of counter-streaming, bi-directional strahl populations is interpreted as the signature of magnetic field lines with both ends connected to the Sun (see, *e.g.*, Pilipp *et al.*, 1987; Lavraud *et al.*, 2009), and is often thought of as a magnetic cloud identifier (Gosling *et al.*, 1987). About half of the MCs observed at 1 AU are at least partly characterized by uni-directional suprathermal electrons (Shodhan *et al.*, 2000; Riley, Gosling, and Crooker, 2004). Such observations have been explained as a result of interchange reconnection at the Sun (Kahler and Lin, 1994; Larson *et al.*, 1997; Crooker *et al.*, 2004; Rouillard *et al.*, 2009). Interchange reconnection at the MC footpoints is schematically displayed in Figures 1c and d, where disconnection of the field line is drawn for only one leg of the MC.

In conclusion, interchange reconnection may naturally occur during the rising phase between open magnetic field lines of a polar coronal hole and a CME such as shown in Figure 1c. But interchange reconnection may also result from the interaction between a CME and the magnetic field lines of a low latitude coronal hole (Baker *et al.*, 2009). Consistent with the Baker *et al.* (2009) case study, this scenario is rather expected during the declining phase and would lead to the poleward transport of open fields, as described in the model of Owens *et al.* (2007) and depicted in Figure 1d.

Using suprathermal electron data for a set of 100 MCs, Crooker *et al.* (2008) recently found that 89% of the MCs that have at least some open fields show open field of a single polarity, while only 11% display mixed open field polarity. Because the opening of the magnetic field is deemed to be the result of interchange reconnection, it was concluded that open magnetic flux transport associated with magnetic cloud systematically occurs in a single direction. However, Crooker *et al.* (2008) could not establish whether or not the sense of flux transport is in agreement with the prediction of Owens *et al.* (2007) for coronal magnetic field reversal during the solar cycle.

3. Summary of Expectations

The results of the present paper come from the simple observation that a combination of the helicity of MCs and information on the pitch angle of suprathermal electrons, both obtained directly from *in-situ* observations, in principle allows us to determine the direction of open field line transport that results from interchange reconnection of MCs at the Sun, as depicted in Figures 1c and d (derived from the model of Owens *et al.* (2007)). For solar cycle 23 with an away polarity in the northern hemisphere at the start of the cycle and active regions following on average Hale's polarity rule, we expect MCs which emerged from new-cycle active regions and interchange reconnect to have the following properties.

- i) Rising phase (Figure 1c): Left-handed helicity MCs (*i.e.*, northern hemisphere) with parallel suprathermal electrons on open field lines (*i.e.*, away polarity) correspond to equatorward open flux transport through interchange reconnection. Expected helicity and polarity are opposite in the southern hemisphere. This implies the closing down and erosion of the polar coronal hole of previous cycle's polarity.
- ii) Solar maximum: Owing to the complex and disordered nature of this phase, flux transport may occur in a number of ways: *i.e.*, this is when the imprints in magnetic clouds are expected to switch.

- iii) Declining phase (Figure 1d): The primary dipole field component of the Sun has changed during the reversal phase. MCs with left-handed helicity (northern hemisphere) and anti-parallel suprathermal electrons on open field lines are expected, together with right-handed helicity and parallel electrons (away polarity) for MC from the southern hemisphere. In this case interchange reconnection would preferentially occur between MCs and isolated (or extension of) coronal holes in the equatorial regions so as to lead to poleward transport of open magnetic fields and complete the formation of the newly established coronal holes.

4. Observations

Figure 2 shows the results of a statistical analysis using the same magnetic cloud list as Crooker *et al.* (2008). We directly used the open field polarities inferred by these authors for each magnetic cloud. For each MC, we also used the helicity information obtained from force-free flux rope fits (Lepping *et al.*, 2006), as available at: http://lepmfi.gsfc.nasa.gov/mfi/mag_cloud_S1.html. The polarities (SN or NS) of the magnetic clouds were also determined. The list used here contains 100 MCs, covering years 1995–2007. Table 1 gives the list of MCs and their properties. Binning by intervals of two years, Figure 2 presents the occurrence statistics of (a) the magnetic (SN/NS) MC polarity, (b) each set of the four possible helicity-polarity (of open magnetic fields within MCs) combinations, (c) the two sets corresponding to either equatorward or poleward open flux transport, and (d) the monthly sunspot occurrence over solar cycle 23. The “away” polarity – “left-handed” helicity (A–L) and “toward” polarity – “right-handed” helicity (T–R) pairs clearly dominate during the rising phase of the cycle, as expected from the model of Figure 1c. In the reversal phase there is no clear tendency, as expected also (see Section 2). During the declining phase there is no clear trend either. This result suggests that footprint exchange does not occur in a systematic way during the declining phase, contrary to expectations from the model of Owens *et al.* (2007) which would imply T–L and A–R pairs to dominate.

It is noted that the occurrence rate of magnetic clouds in the present list is not well correlated with the sunspot occurrence rate. This was already noted by Wu, Lepping, and Gopalswamy (2006) based on the same list of MCs. They showed that if using automated MC identification techniques then the obtained list of “MC-like” structures follows better the solar cycle pattern. In the context of our study, this effect has no significant influence, apart from pointing to the fact that more complete lists of MC-like structures, and for several solar cycles, will be worth future work.

5. Discussion

The present study used a combination of signatures (helicity and polarity) available from *in-situ* MC observations to determine the direction of open flux transport on the Sun that results from interchange reconnection and associated footprint exchange at the legs of MCs. Using the same magnetic cloud list as Crooker *et al.* (2008), our results indicate that, at least for the rising phase of solar cycle 23, MCs undergo interchange reconnection systematically with the open field lines which dominate in their hemisphere of origin, namely the polar coronal holes. If we assume that emerging BMRs follow Hale’s polarity rule then the opening of MCs by interchange reconnection at the Sun is predominantly directed equatorward so that

Table 1 List of magnetic clouds and their properties from Lepping *et al.* (2006) (*cf.* http://lepmfi.gsfc.nasa.gov/mfi/mag_cloud_S1.html) and Crooker *et al.* (2008). T: Toward open magnetic field polarity inferred from uni-directional suprathermal electrons. A: Away open magnetic field polarity. M: Mixed open magnetic field polarity. N: No open magnetic field. L: left-handed MC helicity. R: Right-handed MC helicity. SN: South–north MC-polarity. NS: North–south MC-polarity. U: Unclear MC-polarity.

MC-#	Year	Start-DOY	Start-hour	End-DOY	END-hour	Magnetic field polarity	Helicity	MC-polarity
1	1995	39	5.8	40	0.8	T	L	SN
2	1995	63	10.8	64	3.8	A	L	U
2.2	1995	93	7.8	94	10.8	A	R	NS
3	1995	96	7.3	96	17.8	T	L	U
4	1995	133	10.9	133	16.4	A	L	U
5	1995	234	21.3	235	19.3	A	R	SN
6	1995	291	19.8	293	1.3	T	R	SN
7	1995	350	5.3	350	22.3	T	L	SN
8	1996	148	15.3	150	7.3	A	L	SN
9	1996	183	17.3	184	10.3	A	L	SN
10	1996	220	12.3	221	10.8	T	R	SN
11	1996	359	2.8	360	11.3	T	R	NS
12	1997	10	5.3	11	2.3	M	R	SN
13	1997	41	3.4	41	18.4	A	R	U
14.1	1997	101	5.6	101	19.1	N	R	U
14.2	1997	111	14.5	113	6.5	T	R	SN
15	1997	135	9.1	136	1.1	A	L	SN
16	1997	136	6.1	136	13.9	A	L	NS
17	1997	160	2.3	160	23.3	T	R	SN
18	1997	170	5.1	170	15.9	N	R	U
19	1997	196	8.8	196	23.8	A	L	SN
20	1997	215	14.1	216	1.9	A	L	SN
21	1997	261	0.5	263	12.5	A	R	SN
22	1997	265	0.8	265	17.3	A	L	U
23	1997	274	16.3	275	22.8	N	L	U
24	1997	283	23.8	285	0.8	N	R	SN
25	1997	311	15.8	312	4.3	T	R	SN
26	1997	312	4.9	312	14.9	T	R	NS
27	1997	326	15.8	327	12.3	A	R	NS
28	1998	7	3.3	8	8.3	A	L	U
29	1998	8	14.9	8	21.6	T	R	SN
30	1998	35	4.5	36	22.5	A	L	SN
31	1998	63	14.3	65	6.3	A	L	SN
32	1998	122	12.3	123	17.3	T	L	SN
33	1998	153	10.6	153	15.9	A	L	SN
34	1998	175	16.8	176	21.8	A	L	SN
35	1998	232	10.3	233	19.3	T	R	SN
36	1998	268	10.3	269	13.3	N	L	SN
37	1998	292	5.1	292	14.6	N	R	U

Table 1 (Continued)

MC-#	Year	Start-DOY	Start-hour	End-DOY	END-hour	Magnetic field polarity	Helicity	MC-polarity
38	1998	312	23.8	314	1.3	A	R	SN
39	1999	49	14.3	50	12.3	N	L	U
40	1999	106	20.3	107	21.3	N	L	SN
41	1999	221	10.8	222	15.8	N	L	SN
42	1999	264	21.1	265	5.1	N	L	SN
43	2000	43	17.1	44	0.6	A	L	NS
44.1	2000	52	9.8	53	13.3	T	R	U
44.2	2000	176	8.3	177	20.3	T	L	U
44.3	2000	183	8.8	184	3.3	T	L	U
45	2000	197	6.8	197	14.3	N	L	U
46	2000	197	21.1	198	9.9	N	L	SN
47	2000	210	21.1	211	10.1	T	L	NS
48	2000	214	0.1	214	15.9	A	R	NS
49	2000	225	6.1	226	5.1	A	L	SN
50	2000	262	1.9	262	15.1	N	L	U
51	2000	277	17.1	278	14.1	A	R	NS
52	2000	287	18.4	288	16.9	N	R	NS
53	2000	302	23.3	304	0.3	N	L	SN
54	2000	311	23.1	312	18.1	N	L	SN
55.1	2001	78	23.3	79	18.3	T	L	NS
55.2	2001	79	17.8	81	14.8	T	L	SN
56	2001	94	20.9	95	8.4	N	L	NS
57	2001	102	7.9	102	17.9	N	R	U
58	2001	112	0.9	113	1.4	T	L	NS
59	2001	119	1.9	119	12.9	A	L	SN
60	2001	148	11.9	149	10.4	A	L	SN
61	2001	191	17.3	193	8.8	M	R	SN
62	2001	304	21.3	306	10.3	M	L	SN
63	2001	328	15.8	329	13.3	N	L	U
64	2002	78	22.9	79	15.4	T	R	NS
65	2002	83	3.8	84	22.8	T	R	SN
66	2002	108	4.3	109	2.3	N	R	SN
67	2002	110	11.8	111	16.8	A	L	SN
68	2002	139	3.9	139	23.4	A	R	SN
69	2002	143	23.4	144	16.9	N	L	SN
70	2002	213	11.9	213	22.6	T	R	SN
71	2002	214	7.4	214	21.1	T	L	NS
72.1	2002	246	0.3	246	18.8	M	R	U
72.2	2002	273	22.6	274	11.9	A	L	NS
73	2003	79	11.9	79	22.4	A	R	U
74	2003	168	17.8	169	8.3	T	L	NS
75	2003	191	19.9	192	8.9	N	R	U
76	2003	230	11.6	231	4.4	N	R	U
77	2003	324	10.8	325	2.3	N	R	SN

Table 1 (Continued)

MC-#	Year	Start-DOY	Start-hour	End-DOY	END-hour	Magnetic field polarity	Helicity	MC-polarity
78	2004	95	2.8	96	14.8	M	L	SN
79	2004	204	15.4	204	23.1	A	R	NS
80	2004	206	12.8	207	13.3	N	R	NS
81	2004	242	18.7	243	20.8	T	R	NS
82	2004	313	3.4	313	16.6	A	L	SN
83	2004	314	20.9	315	3.4	A	L	NS
84	2004	315	3.6	315	11.1	A	L	SN
85	2005	135	5.7	135	22.3	N	L	SN
86	2005	140	7.3	141	5.3	A	L	SN
87	2005	163	15.6	164	7.1	A	L	U
88	2005	166	5.8	167	7.8	A	L	SN
89	2005	198	15.3	199	3.8	M	R	NS
90	2005	304	2.9	304	20.4	A	R	NS
91	2005	365	14.8	1	10.8	N	R	SN
92	2006	36	19.1	37	13.1	M	R	NS
93	2006	103	14.8	103	20.8	N	L	SN
94	2006	103	20.6	104	9.9	M	L	NS
95	2006	242	21.1	243	14.9	M	L	NS
96	2006	273	8.6	273	21.6	T	L	NS
97	2006	348	22.8	349	19.8	N	L	SN
98	2007	83	3.1	83	16.9	T	R	SN
99	2007	141	22.9	142	13.6	N	R	NS
100	2007	323	23.4	324	12.9	T	L	NS

open field lines initially located along the equatorward boundary of coronal holes are transported toward lower latitudes, presumably in the equatorial coronal holes which form during the rising phase of solar activity (Benevolenskaya, Kosovichev, and Scherrer, 2001). This is in accord with the observation of a net poleward shift in the peak of coronal green line emissions at the start of a new cycle (Figure 1a). Indeed, the “away” polarity – “left-handed” helicity (A–L) and “toward” polarity – “right-handed” helicity (T–R) pairs clearly peak in the rising phase when the polar coronal holes retreat and their boundaries become suddenly very bright. We suggest that the MCs emerging from the high latitude BMRs interact strongly with the still dominant open field regions of the adjacent polar coronal holes, thus closing down and eroding polar coronal holes during the rising phase. This brightening may be related to energetic particles accelerated during the reconnection process and trapped on loops that now connect the coronal hole boundary with lower-latitude regions (green loops in Figure 1c).

The lack of predominance of “toward” polarity – “left-handed” helicity (T–L) and “away” polarity – “right-handed” helicity (A–R) MCs during the declining phase suggests that interchange reconnection is not occurring as a well-ordered phenomenon during that phase. Interchange reconnection with the dominant polar coronal hole is unlikely because the nearest BMR pole is expected of the same polarity. However, in the framework of Owens *et al.* (2007) model, interchange reconnection may be expected between the equatorward BMR pole and isolated coronal holes of opposite polarity in the equatorial regions. In

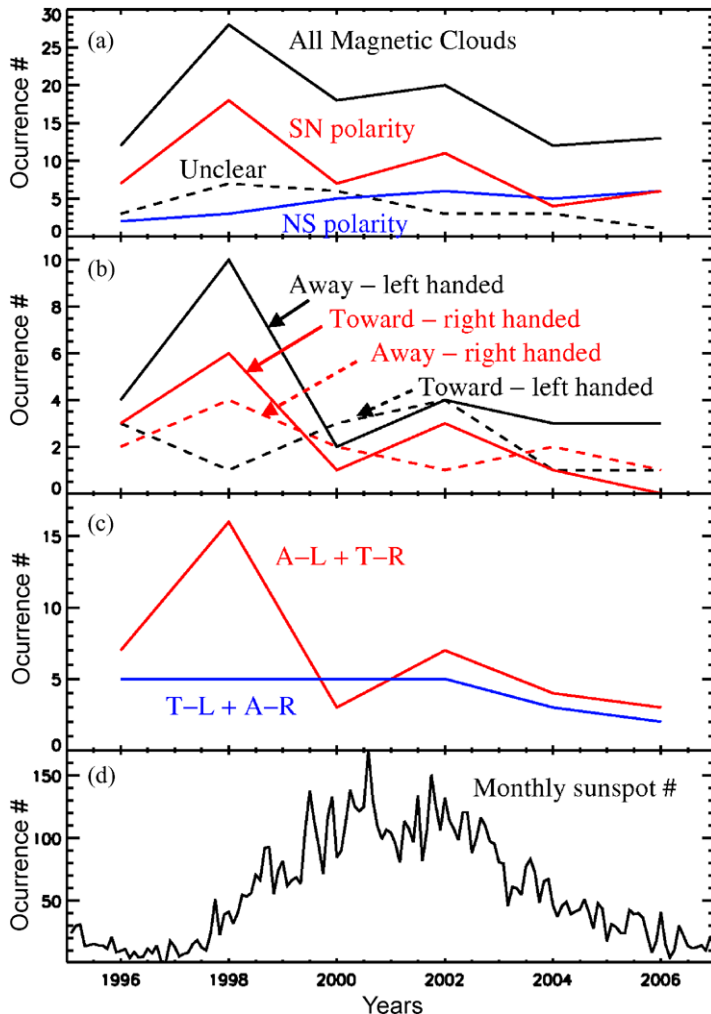


Figure 2 (a) Occurrence statistics of all magnetic clouds during 1995–2007 from the list of Crooker *et al.* (2008) (solid black line), SN-polarity MCs (solid red), NS-polarity MCs (solid blue), and MCs with unclear polarities (dashed black). (b) Occurrence statistics of all four possible pairs of MC open magnetic field polarity – magnetic helicity (color and line-style coding given in panel). (c) Combined occurrence statistics for the “A–L + T–R” pairs, which correspond to equatorward transport in the model of Owens *et al.* (2007), and the “T–L + A–R” pairs, which would correspond to poleward transport. (d) Monthly sunspot occurrence number. Panels (a), (b), and (c) are binned by intervals of two years. The predominance of the A–L + T–R pairs during the rise phase in panel (c) is suggestive of preferential equatorward open flux transport as a result of interchange reconnection at MC footpoints with nearby CHs.

Owens *et al.* (2007) this process leads to completion of the magnetic polarity reversal during the declining phase. Our dataset, however, does not confirm this possibility.

There are several assumptions made in the present paper that ought to be reminded. Although most BMRs follow Hale’s polarity rule, BMRs with wrong polarities emerge occasionally, *i.e.*, MCs with NS-polarity instead of SN-polarity as expected for solar cycle 23 (*cf.* Figure 2b). The assumption that MCs have the appropriate footpoint config-

uration (in terms of the polarity and latitude of the leading and trailing poles) is only true for 75% of magnetic clouds (Bothmer and Rust, 1997; Bothmer and Schwenn, 1998; Rees and Forsyth, 2003). The helicity law is hemispheric-dependent about the solar rotation axis, while the leading-trailing pole law (in terms of sign and latitude) is rather expected to be hemispheric-dependent about the magnetic dipole axis. Therefore, the relationship we draw here should work best when the dipole axis and magnetic axis are close to being aligned, which may not be a good assumption during the declining phase. There are several CME models, and likely several actual CME release mechanisms, *e.g.*, tether cutting (see, *e.g.*, Moore *et al.*, 2001), magnetic breakout (Antiochos, DeVore, and Klimchuk, 1999), streamer blowout (see, *e.g.*, Wang *et al.*, 2000), trans-equatorial filament eruptions (see, *e.g.*, Delannée and Aulanier, 1999; Pevtsov, 2000), or polar crown filament-related CMEs (Gopalswamy *et al.*, 2010). Only some of those models would be compatible with the hemisphere-asymmetric interchange reconnection process discussed in the present paper. Further knowledge of actual and dominant CME release mechanisms would be required to determine the impact on the present results. Although it is often assumed that uni-directional suprathermal electrons in magnetic clouds signal the occurrence of interchange reconnection in the lower corona, it should be noted that the possibility of magnetic cloud erosion in the interplanetary medium has so far been little studied (Dasso *et al.*, 2007; Tian *et al.*, 2010).

We finally point out the fact that the models of open flux transport described by Fisk and Schwadron (2001) and Wang and Sheeley (2003) differ from the model of Owens *et al.* (2007) in that the total open flux transport associated with CMEs is not a major contributor to the global coronal field reversal. Fisk and Schwadron (2001) explain this restructuring based on reconnection between open coronal hole fields and streamer belt closed loops. Wang and Sheeley (2003) used a flux-transport model to show that the polar reversal is the result of BMR loops opening and transport toward the polar regions via a diffusion process and poleward meridional flows. The present results suggest that the process of removing the open field lines at high latitudes during the rising phase is, in addition and at least in part, the result of CME activity, interchange reconnection, and associated equatorward open magnetic flux transport.

Acknowledgements We are grateful to Eva Robbrecht and Yi-Ming Wang for discussions and provision of the photospheric maps and simulated green line emissions. We are also grateful to R. Lepping for making the MC helicity list used here available to the community.

References

- Antiochos, S.K., DeVore, C.R., Klimchuk, J.A.: 1999, *Astrophys. J.* **510**, 485.
- Babcock, H.W.: 1961, *Astrophys. J.* **133**, 572.
- Baker, D., Rouillard, A.P., van Driel-Gesztelyi, L., Démoulin, P., Harra, L.K., Lavraud, B., *et al.*: 2009, *Ann. Geophys.* **27**, 3883.
- Benevolenskaya, E.E., Kosovichev, A.G., Scherrer, P.H.: 2001, *Astrophys. J. Lett.* **554**, 107.
- Bothmer, V., Rust, D.M.: 1997, In: Crooker, N., Joselyn, J.A., Feynman, J. (eds.) *Coronal Mass Ejections, AGU Geophys. Monogr.* **99**, 139.
- Bothmer, V., Schwenn, R.: 1998, *Ann. Geophys.* **16**, 1.
- Burlaga, L.F., Klein, L., Sheeley, N.R., Michels, D.J., Howard, R.A., Koomen, M.J., Schwenn, R., Rosenbauer, H.: 1982, *Geophys. Res. Lett.* **9**, 1317.
- Cane, H.V., Richardson, I.G.: 2003, *J. Geophys. Res.* **108**(A4), SSH 6-1.
- Chandra, R., Pariat, E., Schmieder, B., Mandrini, C.H., Uddin, W.: 2010, *Solar Phys.* **261**, 127.
- Cohen, O., Attrill, G.D.R., Schwadron, N.A., Crooker, N.U., Owens, M.J., Downs, C., Gombosi, T.I.: 2010, *J. Geophys. Res.* **115**, A10104.
- Crooker, N.U., Kahler, S.W., Larson, D.E., Lin, R.P.: 2004, *J. Geophys. Res.* **109**, A03108.

- Crooker, N.U., Kahler, S.W., Gosling, J.T., Lepping, R.P.: 2008, *J. Geophys. Res.* **113**, A12107.
- Dasso, S., Nakwacki, M.S., Démoulin, P., Mandrini, C.H.: 2007, *Solar Phys.* **244**, 115.
- Delannée, C., Aulanier, G.: 1999, *Solar Phys.* **190**, 107.
- Dikpati, M., Gilman, P.A., de Toma, G., Ulrich, R.K.: 2010, *Geophys. Res. Lett.* **37**, L14107.
- Edmondson, J.K., Antiochos, S.K., DeVore, C.R., Lynch, B.J., Zurbuchen, T.H.: 2010, *Astrophys. J.* **714**, 517.
- Fisk, L.A., Schwadron, N.A.: 2001, *Astrophys. J.* **560**, 425.
- Gopalswamy, N., Lara, A., Yashiro, S., Howard, R.A.: 2003, *Astrophys. J. Lett.* **598**, 63.
- Gopalswamy, N., Akiyama, S., Yashiro, S., Mäkelä, P.: 2010, In: Hasan, S.S., Rutten, R.J. (eds.) *Magnetic Coupling between the Interior and Atmosphere of the Sun*, Springer, Berlin, 289.
- Gosling, J.T.: 1990, In: Russell, C.T., Priest, E.R., Lee, L.C. (eds.) *Physics of Magnetic Flux Ropes*, AGU Geophys. Monogr. **58**, 343.
- Gosling, J.T., Baker, D.N., Bame, S.J., Feldman, W.C., Zwickl, R.D., Smith, E.J.: 1987, *J. Geophys. Res.* **92**, 8519.
- Hale, G.E., Nicholson, S.B.: 1925, *Astrophys. J.* **62**, 270.
- Kahler, S., Lin, R.P.: 1994, *Geophys. Res. Lett.* **21**, 1575.
- Larson, D.E., et al.: 1997, *Geophys. Res. Lett.* **24**, 1911.
- Lavraud, B., Borovsky, J.E.: 2008, *J. Geophys. Res.* **113**, A00B08.
- Lavraud, B., Gosling, J.T., Rouillard, A.P., Fedorov, A., Opitz, A., Sauvaud, J.-A., et al.: 2009, *Solar Phys.* **256**, 379.
- Lavraud, B., Opitz, A., Gosling, J.T., Rouillard, A.P., Meziane, K., Sauvaud, J.-A., Fedorov, A., Dandouras, I., Génot, V., Jacquay, C.: 2010, *Ann. Geophys.* **28**, 233.
- Leighton, R.B.: 1969, *Astrophys. J.* **140**, 1547.
- Lepping, R.P., Berdichevsky, D.B., Wu, C.-C., Szabo, A., Narock, T., Mariani, F., Lazarus, A.J., Quivers, A.J.: 2006, *Ann. Geophys.* **24**, 215.
- Low, B.C.: 2004, In: Pap, J.M., Fox, P. (eds.) *Solar Variability and Its Effects on Climate*, AGU Geophys. Monogr. **141**, 51.
- Moore, R.L., Sterling, A.C., Hudson, H.S., Lemen, J.R.: 2001, *Astrophys. J.* **552**, 833.
- Mulligan, T., Russell, C.T., Luhmann, J.G.: 1998, *Geophys. Res. Lett.* **25**, 2959.
- Owens, M.J., Schwadron, N.A., Crooker, N.U., Hughes, W.J., Spence, H.E.: 2007, *Geophys. Res. Lett.* **34**, L06104.
- Pevtsov, A.A.: 2000, *Astrophys. J.* **531**, 553.
- Pilipp, W.G., Migenrieder, H., Montgomery, M.D., Mühlhäuser, K.-H., Rosenbauer, H., Schwenn, R.: 1987, *J. Geophys. Res.* **92**, 1093.
- Riley, P., Gosling, J.T., Crooker, N.U.: 2004, *Astrophys. J.* **608**, 1100.
- Rees, A., Forsyth, R.J.: 2003, *Geophys. Res. Lett.* **30**(19), ULY4-1.
- Robbrecht, E., Wang, Y.-M., Sheeley, N.R., Rich, N.B.: 2010, *Astrophys. J.* **716**, 693.
- Rouillard, A.P., Savani, N., Davies, J.A., Lavraud, B., Farsyth, R.J., Morley, S.K., et al.: 2009, *Solar Phys.* **256**, 307.
- Rust, D.M.: 1994, *Geophys. Res. Lett.* **21**, 241.
- Schrijver, C.J., DeRosa, M.L., Title, A.M.: 2002, *Astrophys. J.* **577**, 1006.
- Sheeley, N.R., Wang, Y.-M., Harvey, J.W.: 1989, *Solar Phys.* **119**, 323.
- Shodhan, S., Crooker, N.U., Kahler, S.W., Fitznerreiter, R.J., Larson, D.E., Lepping, R.P., Siscoe, G.L., Gosling, J.T.: 2000, *J. Geophys. Res.* **105**, 27261.
- Tian, H., Yao, S., Zong, Q., He, J., Qi, Y.: 2010, *Astrophys. J.* **720**, 454.
- Wang, Y.-M., Sheeley, N.R.: 1989, *Solar Phys.* **124**, 81.
- Wang, Y.-M., Sheeley, N.R.: 2003, *Astrophys. J.* **599**, 1404.
- Wang, Y.-M., Nash, A.G., Sheeley, N.R.: 1989a, *Astrophys. J.* **347**, 529.
- Wang, Y.-M., Nash, A.G., Sheeley, N.R.: 1989b, *Science* **245**, 712.
- Wang, Y.-M., Sheeley, N.R., Hawley, S.H., Kraemer, J.R., Brueckner, G.E., Howard, R.A., et al.: 1997, *Astrophys. J.* **485**, 419.
- Wang, Y.-M., Sheeley, N.R., Socker, D.G., Howard, R.A., Rich, N.B.: 2000, *J. Geophys. Res.* **105**, 25133.
- Wang, Y.-M., Robbrecht, E., Rouillard, A.P., Sheeley, N.R., Thernisien, A.F.R.: 2010, *Astrophys. J.* **715**, 39.
- Webb, D.F., Howard, R.A.: 1994, *J. Geophys. Res.* **99**, 4201.
- Wu, C.-C., Lepping, R.P., Gopalswamy, N.: 2006, *Solar Phys.* **239**, 449.
- Zwickl, R.D., Asbridge, R.J., Bame, S.J., Feldman, W.C., Gosling, J.T., Smith, E.J.: 1983, In: Neugebauer, M. (ed.) *Solar Wind Five*, NASA CP-2280, 711.